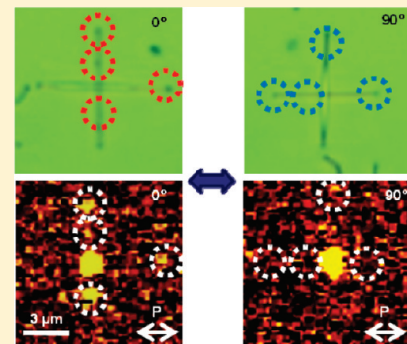


Raman Markers from Silver Nanowire Crossbars

Sehoon Chang, Hyunhyub Ko, Ray Gunawidjaja, and Vladimir V. Tsukruk*

School of Materials Science and Engineering, Georgia Institute of Technology, Atlanta, Georgia 30332, United States

ABSTRACT: We fabricated silver nanowire crossbars partially decorated with silver nanoparticles via a double-step transversal capillary transfer microprinting approach and demonstrated their polarization-dependent surface-enhanced Raman scattering (SERS) properties. We demonstrated that SERS intensity of nanowire junctions and nanowire–nanoparticle junctions can be turned on/off on demand by the rotation of the polarization plane, which excites specific transversal plasmon resonances and initiates selective excitation/suppression of central and auxiliary nanostructured junctions. We suggest that massive fabrication of such addressable crossbar nanojunctions is important for exploiting these SERS markers for chemical and biological detection assays.



INTRODUCTION

One dimensional metal nanostructures with the capability of guiding electromagnetic energy are attractive for nanoscale optical devices and circuits.^{1,2} These nanostructures can be also excellent candidates for Raman markers that exploit surface-enhanced Raman scattering (SERS) phenomena.^{3–9} One-dimensional nanostructures show promising capabilities for guiding and confining the exciting light in nanogaps (“hot spots”), providing dramatically enhanced local electromagnetic field and coupling of localized surface plasmon resonances. To explore this important phenomenon, a number of different noble metal nanostructures have been fabricated, assembled, and synthesized, and some have been suggested as prospective Raman markers for chemical and biological detection.^{10–16}

Several recent examples of label-free Raman markers from metallic/bimetallic nanostructures include silver nanowires and their bundles,^{17–19} silver nanocubes and nanoplates,^{20,21} rods with fabricated gaps,²² nanodumbbells,²³ gold nanowire–gold nanoparticles,^{24,25} crossed gold nanowires,²⁶ ZnO nanowire–silver nanoparticle hybrid nanotrees,^{27,28} and silver–gold nanocobs.²⁹ Efficient SERS phenomena have been observed for crossed silver nanowires and for prefabricated bundles with localized nanojunctions. Moreover, intriguing polarization-dependent SERS phenomenon that can be utilized for waveguiding and controlled longitudinal surface plasmon localization have been demonstrated for silver nanowires decorated with multiple nanoparticles and their clusters.³⁰ However, examples of single-nanoparticle-based hot spots with SERS appearance tuned by the polarization-dependent excitation conditions are rarely demonstrated.

Here, we report on remarkable properties of crossbars of silver nanowires partially decorated with spherical silver nanoparticles associated with SERS hot spots with optical turning on/off mediated by polarization conditions at a nanojunction. Massive fabrication can be achieved via a double-step transversal capillary

transfer microprinting approach. Such addressable on/off behavior is controlled by the rotation of the polarization plane which excites transversal plasmon resonances and initiates selective excitation of SERS hot spots at different locations. Moreover, we demonstrated the possibility of massive fabrication of such junctions by simple, double-step capillary transfer lithography,^{31,32} which might open a path for large-scale assay applications.

RESULTS AND DISCUSSION

The silver nanowires exploited in this study were obtained according to a well-established procedure with optimization of chemical composition to obtain predominantly nanowires with a minor content of nanoparticles (see Experimental Section).³³ The resulting product was a mixture of silver nanowires and spherical nanoparticles. The silver nanowires were isolated from the spherical nanoparticles by multiple centrifugation (3000 rpm) and redispersion in methanol.

For the purpose of this experiment, the silver nanowires were only exposed twice to the centrifugation and redispersion cycle to maintain certain concentration of spherical silver nanoparticles, which gives the silver nanowires/spherical silver nanoparticles mixture.^{34–39} These 5 μm long silver nanowires with a diameter of 120 nm, due to the synthetic procedure, are capped with a monolayer of polyvinylpyrrolidone (PVP), as suggested earlier.⁴⁰ Indeed, a direct comparison of TEM (visualizing only silver nanowires) and AFM (visualizing nanowires with shell) data shows that the upper limit of the PVP coating thickness could not exceed 5 nm (not shown).

We used the sacrificial double-step microprinting approach with polymer micropatterns as guided templates for the deposition

Received: September 29, 2010

Revised: February 8, 2011

Published: March 02, 2011

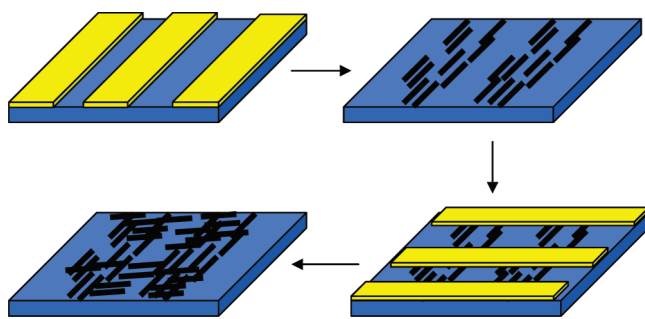


Figure 1. Fabrication of a crossbar array of silver nanowires using sacrificial polymer micropatterns as guided templates in the double-step transversal capillary transfer microprinting and orientation process.

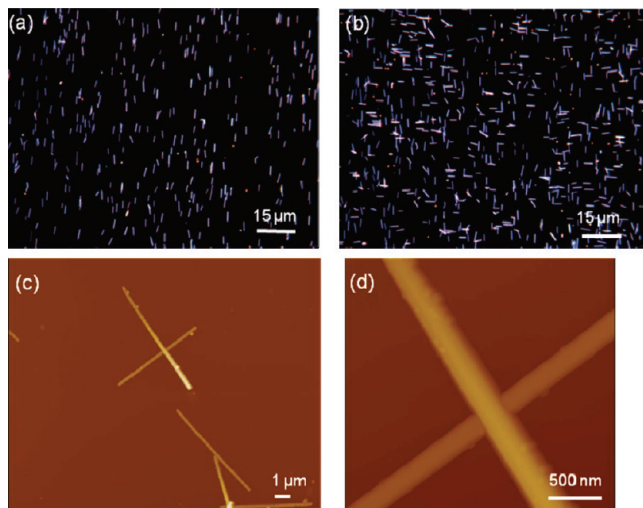


Figure 2. Dark-field optical micrographs of (a) uniformly oriented silver nanowires and (b) an array of orthogonal nanowires. (c,d) AFM images of individual silver nanowires and crossbars.

of silver nanowires to prepare crossbar arrays of silver nanowires on a silicon substrate (Figure 1). To yield a highly oriented array, silver nanowire solution (1–3 mg/mL in methanol) was drop-casted onto the array of narrow channels composed of a sacrificial polystyrene (PS) micropattern (ridges with 3 μm periodicity and 1 μm height), resulting in parallel arrays of silver nanowires. The 1 μm thick sacrificial PS micropattern was deposited on the silicon substrate by a polydimethylsiloxane (PDMS) stamp. After deposition of silver nanowires, the PS pattern was lifted off by toluene, leaving patterned stripe arrays of highly oriented silver nanowires (Figure 2a). We repeated the process of PS micropatterns perpendicular to the first layer of silver nanowire arrays to prepare crossed arrays of silver nanowires.⁴¹

By repeating this template-orientation procedure in an orthogonal direction, a massive silver nanowire array with orthogonally oriented silver nanowire pairs of L and T shapes as well as crossbars can be formed (Figure 2b). Overall, more than 40% of all silver nanowires participate in the formations of junctions between perpendicular nanowires of different types.

Individual crossbars are composed of two perpendicular silver nanowires with one nanowire crossing another, as visible from SEM and AFM images (Figures 2 and 3). Cross-sectional analysis of crossbars in the junction point shows that top and bottom nanowires are not significantly deformed after the formation of

crossbars and stay within $\pm 5\%$ (Figure 3c). Therefore, PVP coating is not significantly deformed by slightly bend the top nanowire and allow access of external analytes to the central junction. Occasionally, silver nanoparticles attached to the silver nanowires can be also observed on corresponding SEM and AFM images (Figures 2 and 3).

Raman spectra of bulk PVP, which is a coating material for silver nanowires, showed characteristic bands in the 740–1650 cm^{-1} range, corresponding to ring breathing vibrations, and a strong peak at 2925 cm^{-1} , which corresponds to CH_2 asymmetric stretching (Figure 4).⁴⁰ Raman spectra of PVP-coated silver nanowires show a strong peak at 232 cm^{-1} due to Ag–O stretching vibration. A strong peak at 1599 cm^{-1} showed up as a result of SERS (Figure 4).⁴² This characteristic band with high intensity was utilized in this study for Raman micromapping.

Figure 5a displays an example of such measurements, which include optical images of a selected nanowire crossbar. Optical images of the silver nanowire crossbars show the presence of nanoparticles located along the nanowires as well as in the vicinity of the crossbar. The corresponding SERS micromapping for this selected silver nanowire crossbar at different orientations of this crossbar with respect to the polarization direction (always horizontal) is shown in Figure 5b. Raman scattering collected with high resolution (50 nm per pixel, $\lambda = 514 \text{ nm}$) at this polarization shows the strongest central spot (1), which corresponds to the crossbar nanojunction (Figure 5). This location represents the most intense hot spot caused by coupled transversal plasmon resonances of bottom and top nanowires.

A characteristic pattern of other bright spots corresponds to the locations of silver nanoparticles along the vertical nanowires (three spots in the middle section, points 2–4) (Figure 6). Low-intensity spots are also associated with left and right (point 5) tips of the horizontal nanowire (Figure 6).

Rotation of the polarization plane with respect to the crossbar changes their scattering intensities dramatically (Figure 5b). Raman scattering shows the central brightest hot spot, which corresponds to the junction of the nanowires at different polarization orientations with significant increase at 45° polarization orientation (Figure 5b). The intensity of this hot spot changes somewhat at different polarization orientations due to background scattering and fluorescence with overall intensity gradually decreasing due to continuous photoinitiated pyrolysis during long-time collection of images (from left to right in Figure 5c).^{43–45} It is worth noting again that all images presented here are collected from a central junction (single pixel size of 50 nm), thus reflecting highly localized point excitation and not integrated Raman scattering averaged over a large surface area.

In contrast to overall intensity, the shape of the double band within 1400–1600 cm^{-1} does not change much at different polarization orientations.⁴⁶ On the other hand, a characteristic cross-shaped pattern of localized hot spots at 0° can be recognized at 45° and partially at 135° as well as 180°, although with lower intensities (Figure 5). However, the cross-shaped pattern disappears for the 90° polarization orientation.

The polarization-dependent appearance and disappearance of the different hot spots can be understood considering recent results on SERS behavior of one-dimensional structures. Indeed, it has been demonstrated that decorating silver nanowires with nanoparticles results in highly localized plasmon resonances along the nanowires.⁴⁷ It has been also observed that the excitation of transversal plasmon resonances in decorated silver

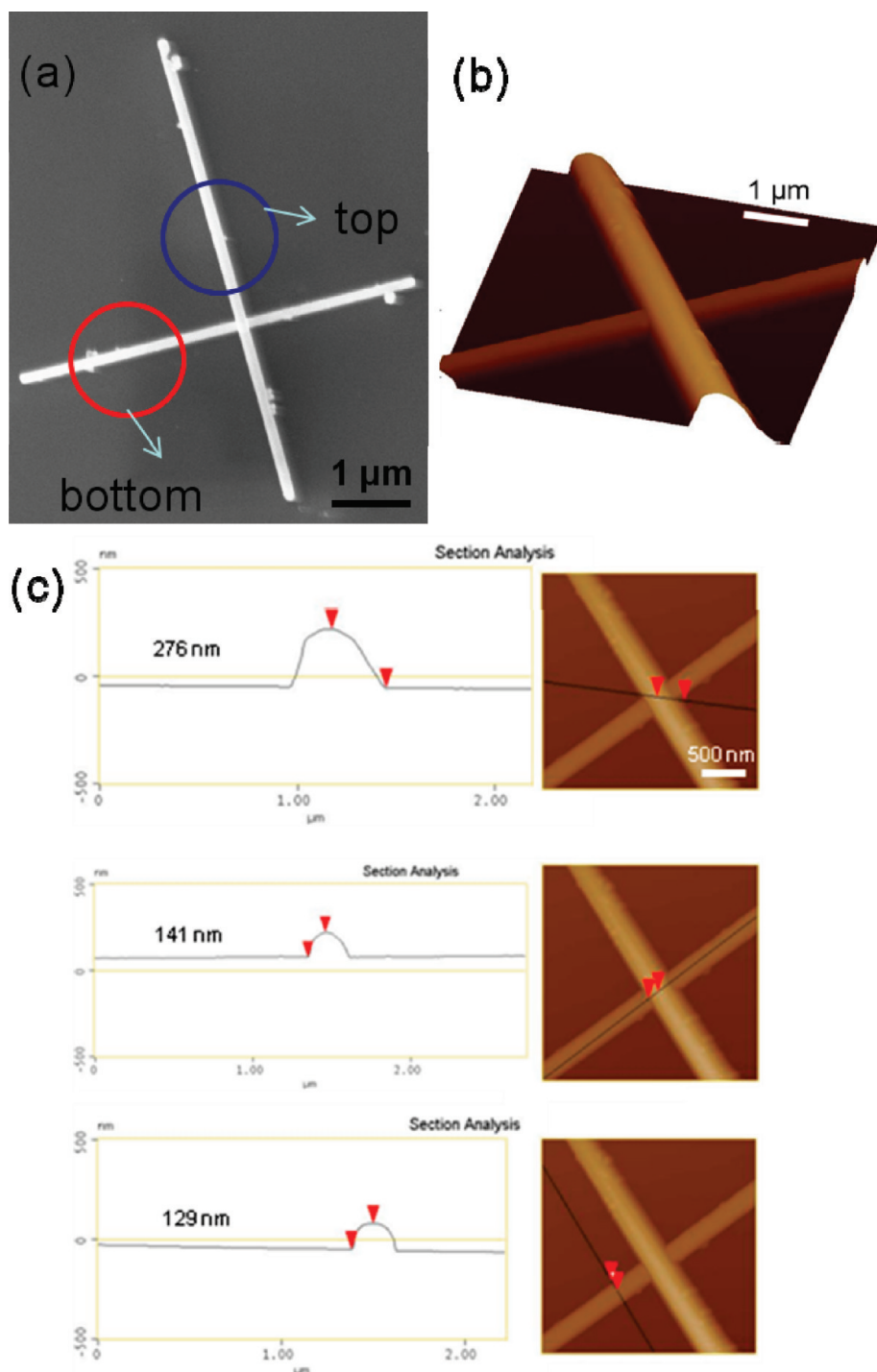


Figure 3. (a) SEM of a single silver nanowires crossbar with attached nanoparticles and (b) 3D AFM images of central junction of silver nanowires crossbar, which allows one to distinguish top and bottom nanowires with corresponding cross sections (c).

nanowires for polarization perpendicular to the long axis causes a significant polarization-dependent SERS effect.³⁰

In the case of the crossbars locally decorated with silver nanoparticles, we can distinguish two very different polarization-dependent phenomena. Polarization-independent characteristics of the central hot spot with the highest intensity can be caused by complementary contributions of coupled orthogonal transversal plasmon resonances at different polarization orientations (Figure 6). If the hot spot is formed at a nanoparticle—

nanowire gap, strong polarization dependence should be observed with strongest Raman intensity observed if the direction of polarization is perpendicular to the nanowires long axis.³⁰ These differences should cause a peculiar polarization-dependent behavior of crossbars, which is very different from the behavior of single nanowires and their bundles. Namely, this unique feature is an unchanged central hot spot at the crossbar junction combined with strong polarization-dependent auxiliary hot spots along nanowires, as illustrated in Figure 5. The pattern observed in

the experiment discussed here can be explained by lateral attachment of the associated silver nanoparticles (points 2–4) to vertical nanowires and nanoparticle (point 5) attached to the nanowire's tip (Figure 6). In this schematic, white arrows show different directions of localized transversal plasmon resonances between nanowires and nanoparticles as well as at the junction of two different crossbar orientations, which correspond to two situations with 0° and 90° polarizations, as presented in Figure 6.

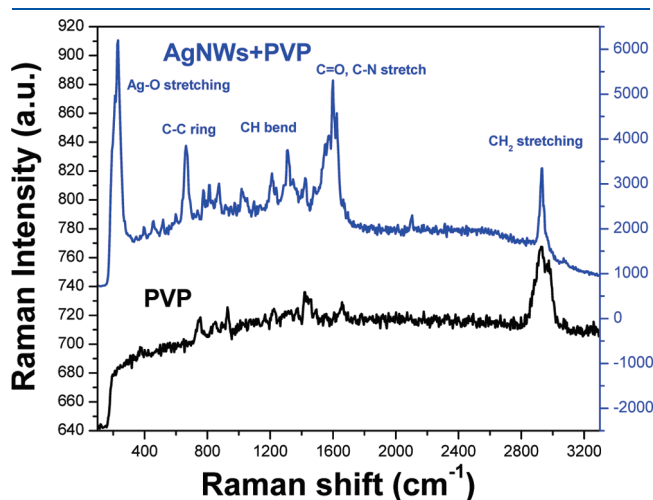


Figure 4. Raman spectra of bulk PVP material and silver nanowires coated with PVP.

We further demonstrate the polarization-dependent SERS results for other shapes of crossbars for which the horizontal nanowire is located on top of the vertical nanowire in Figure 7. SEM images of the crossbars confirm the location of nanoparticles, which is exactly corresponding to the SERS hot spots, as indicated in Figure 8 and illustrated in Raman micromapping in Figure 9. Each Raman spectra from the silver nanowire crossbar is demonstrated in Figure 9, and the red circles correspond to the different hot spots. Overall, these results reveal polarization-independent characteristics of the central hot spot caused by coupled transversal plasmon resonances of the bottom and top nanowires.

At different polarization directions, the relative Raman intensities at the central junction of the nanowire crossbar is maintained as the same intensity as shown in Figure 7a (point 1). On the other hand, the SERS at the junction of nanowire and spherical nanoparticles shows the polarization-dependent characteristics. At the hot spots marked as red circles in the SEM images (Figure 7a, points 2,3), the relative Raman intensities from PVP coating at the junction between nanowire and nanoparticle are observed to be enhanced as the polarization direction is changed due to the coupling with the silver nanoparticles (Figure 7b). The stronger Raman intensities were also observed when the direction of polarization is perpendicular to the nanowires long axis. Lower Raman enhancement is observed in the case of the junction between attached nanoparticles and nanowire (Figure 7a, point 4) and if the laser polarization direction is perpendicular to the nanoparticle–nanowire gap (Figure 7b). The schematic of the hot spots (red circles) of the silver nanowire crossbar with attached nanoparticles and

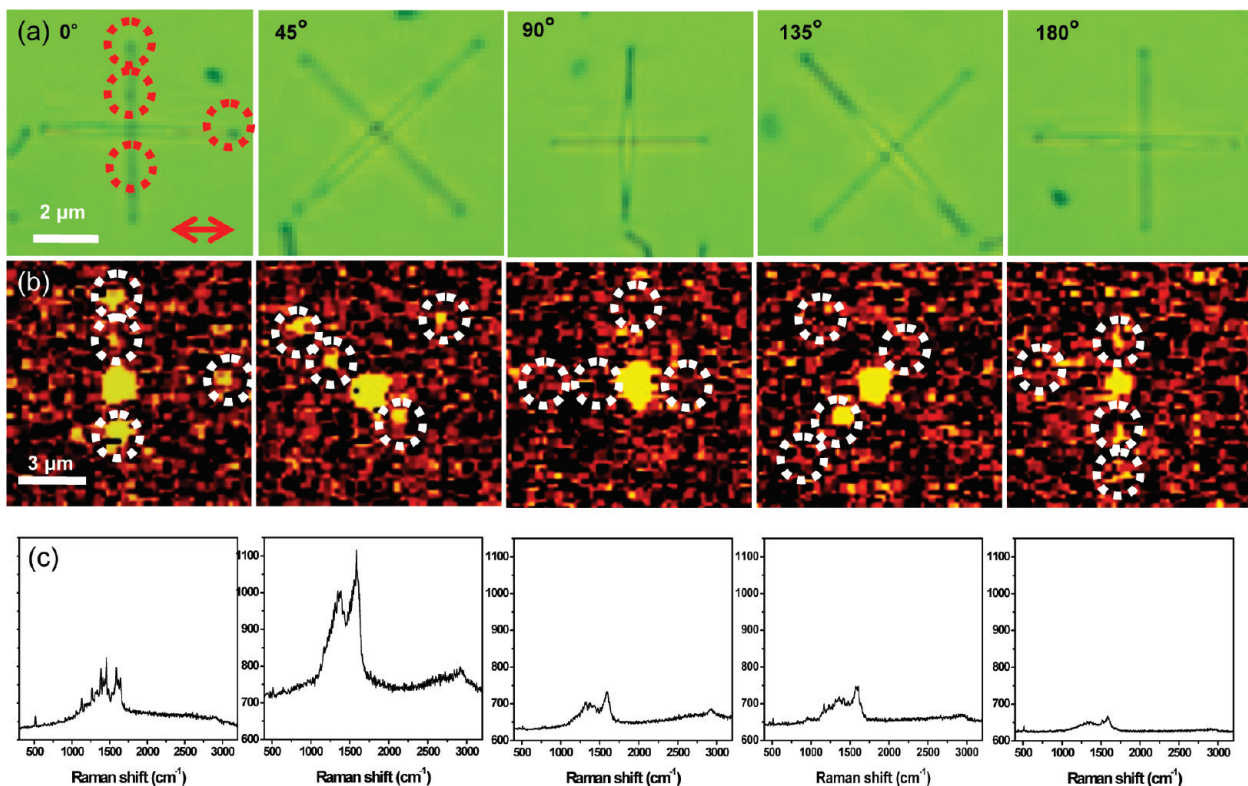


Figure 5. (a) Optical micrographs, (b) Raman micromapping of crossbars with different orientation (dashed circles indicating attached silver nanoparticles on silver nanowires and corresponding hot spots, polarization is horizontal for all images), and (c) corresponding Raman spectra of central junction from images b.

nano particle dimers also correlates with variable SERS intensities at different polarization directions (Figure 8).

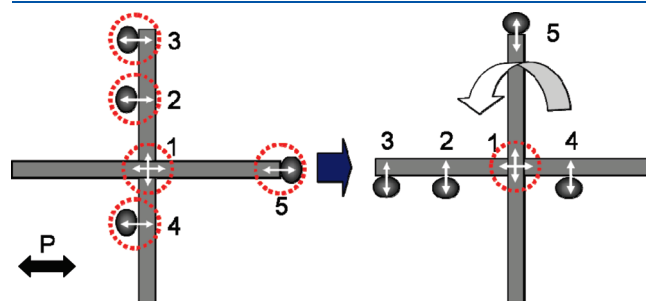


Figure 6. Schematic of the different directions of plasmon resonances of silver nanowires with attached nanoparticles at different orientations; polarization is horizontal.

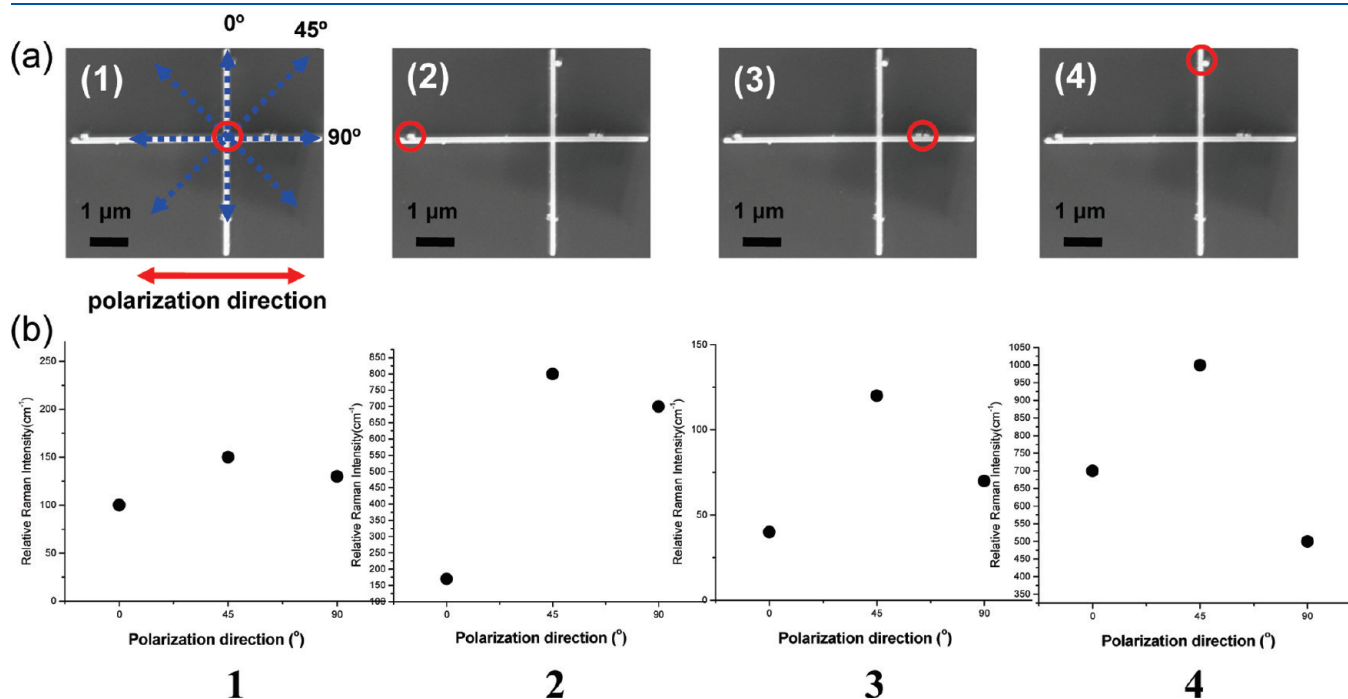


Figure 7. (a) Hot spots (circles) of silver nanowires crossbar with attached nanoparticles with different orientations (polarization is horizontal), circles indicating hot spots at different crossbar orientations and numbers corresponding to selected points in part a. (b) Relative Raman intensity of 1599 cm^{-1} at each hot spot (points 1–4 from part a) of silver nanowire crossbars at different polarization directions.

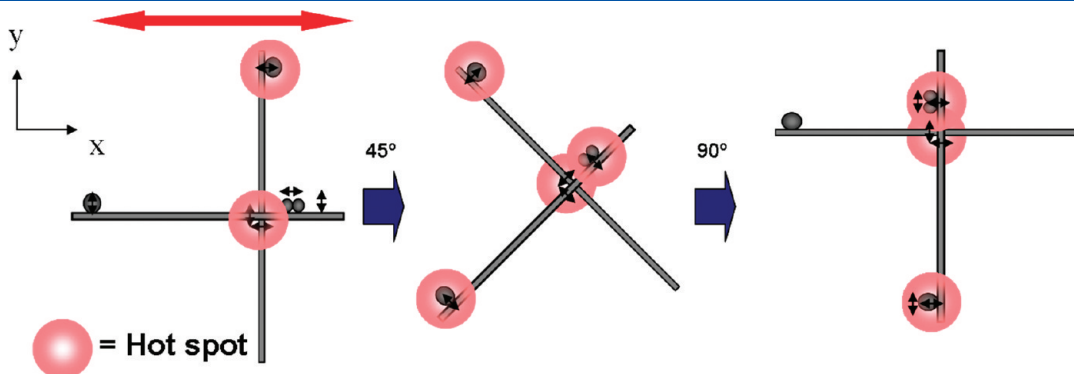


Figure 8. Schematic of hot spots (circles) of silver nanowire crossbar attached with nanoparticles at different crossbar orientations.

We exposed our silver nanowire crossbar with silver nanoparticles to a well-known Raman analyte, Rhodamine 6G (R6G), to study the SERS polarization dependence with higher angular resolution than that demonstrated for Raman mapping above. For these measurements, the silver nanowire crossbars with silver nanoparticles deposited on Si substrate were immersed in an aqueous solution of 10^{-5} M R6G, rinsed thoroughly with Nanopure water, and dried. SERS spectra from the silver nanowire crossbar junction and the silver nanowire–nanoparticle junction were collected with 1 s exposure time with three rounds of accumulations to ensure high signal-to-noise ratio (Figure 10). Characteristic Raman bands of R6G (1360 , 1504 , and 1644 cm^{-1}) from aromatic benzene rings were strongly enhanced at the nanowire crossbar junction and visible at the SERS spectrum (Figure 10a). The SEM image clearly shows the silver nanowire crossbar junction and the silver nanowire–nanoparticle junction, which corresponds exactly to the spectra collected and analyzed (Figures 10 and 11).

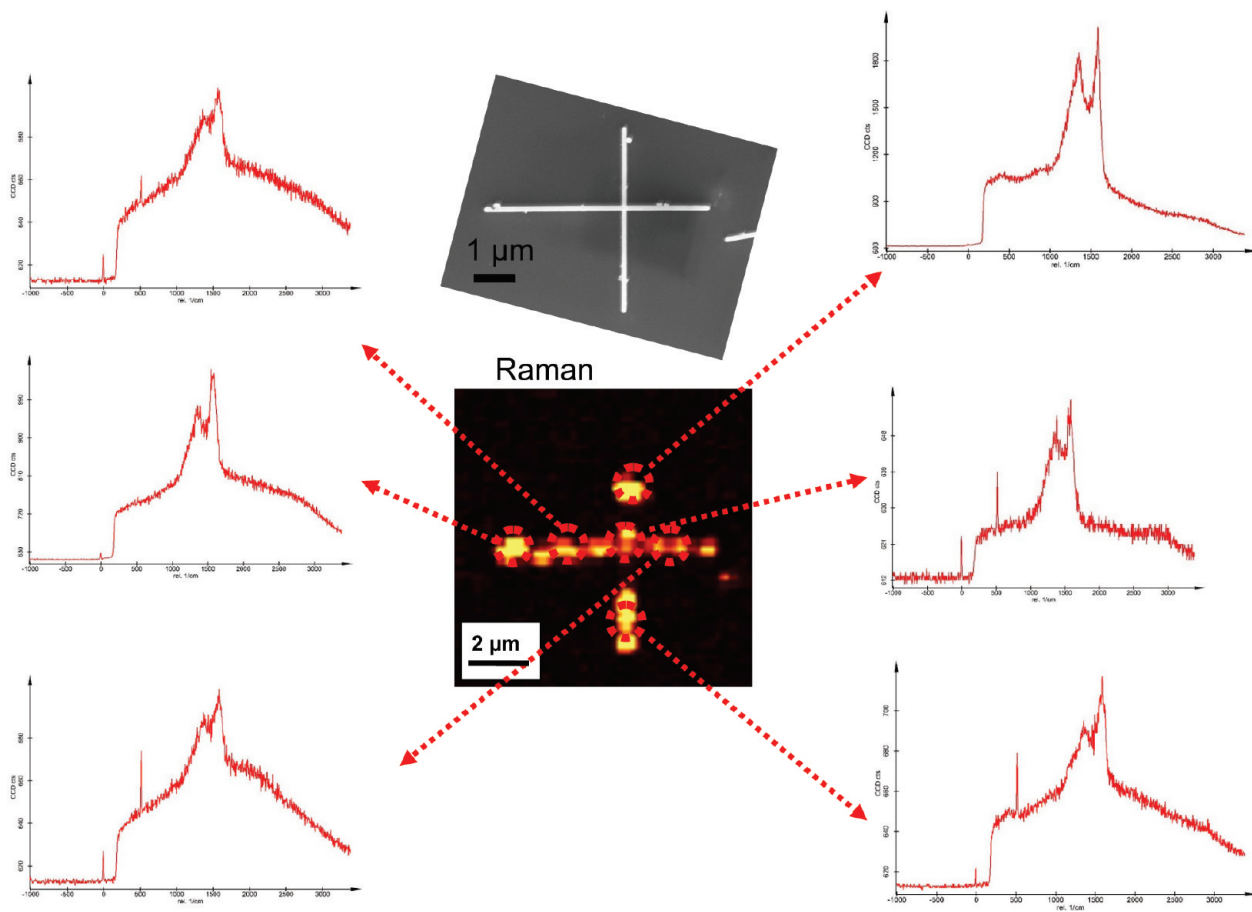


Figure 9. Raman spectra of a crossbar of silver nanowires; red circles correspond to the different hot spots with corresponding Raman spectra shown in separate plots.

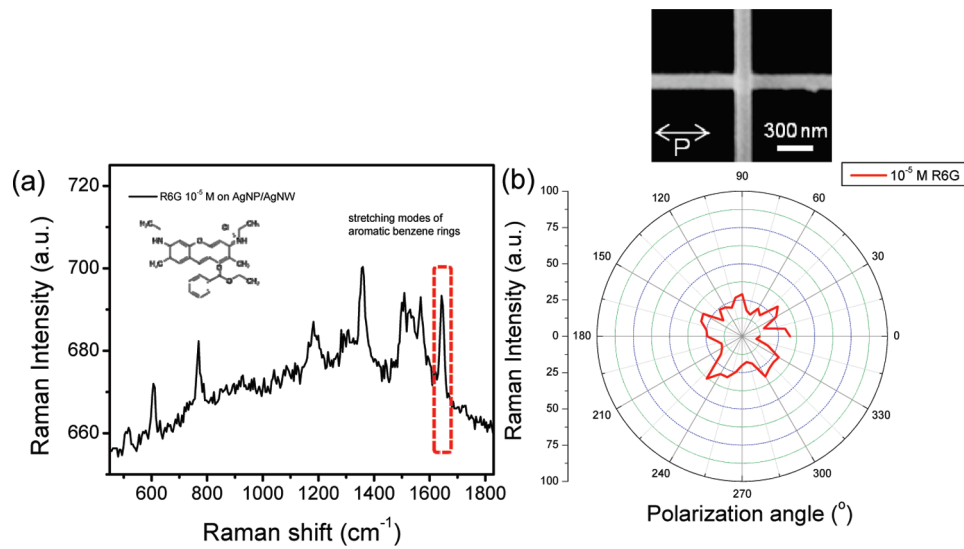


Figure 10. (a) Raman spectra of 10^{-5} M of R6G on silver nanowire crossbar junction and (b) the relative Raman intensity of 1644 cm^{-1} from the silver nanowire crossbar junction at different polarization directions; the inset shows the specific crossbar tested here at a particular orientation (0°).

The relative intensity of the specific Raman band at 1644 cm^{-1} was monitored and plotted at each 10° of polarization orientation, as presented in polar diagrams in Figures 10b and 11b. As was observed, the relative Raman intensities of selected band at the central junction of nanowire crossbar maintained near

constant intensity at different polarization directions within $\pm 30\%$ (Figure 10b). This modest and random variation confirms the fact that the two crossing nanowires create coupling conditions that are polarization independent, as was reported above from Raman mapping with lower angular resolution.

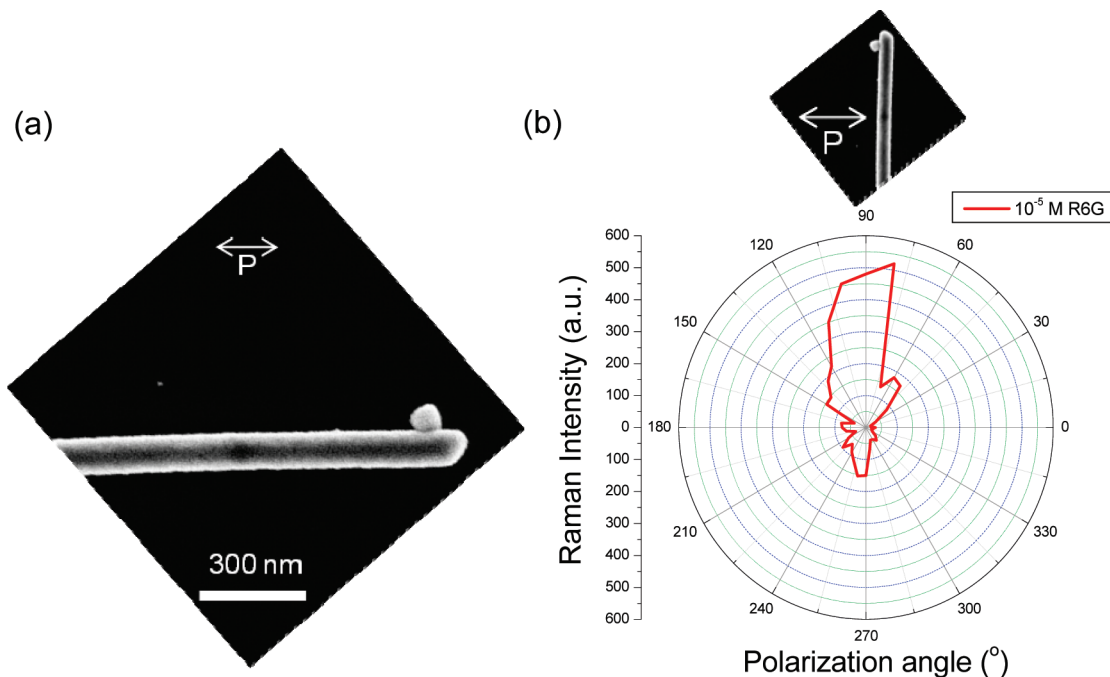


Figure 11. (a) High-resolution SEM image of the junction between silver nanoparticle and nanowire and (b) the relative Raman intensity of 1644 cm^{-1} from the silver nanowire–nanoparticle junctions at different polarization directions; the insets show the specific nanowire–nanoparticle end tested here at two particular orientations (90° and 0°).

However, for a single nanoparticle attached to the nanowire, a strong polarization dependency has been observed (Figure 11). As the polarization angle changes to become perpendicular to the junction between silver nanoparticle and silver nanowire, the Raman intensity increases up to 15 times due to the coupling of nanostructures (Figure 11b).³⁷ As the polarization becomes close to parallel to the junction of the nanoparticle and nanowire (see the inset in Figure 11b), the relative Raman signal intensity decreases dramatically to close to the background level. It is worth noting that the gradual decrease of the overall relative Raman intensity with measuring time reflects the gradual deterioration of organic molecules during the continuous exposure to laser illumination, a common phenomenon observed for similar nanostructures.³⁰ However, overall it is apparent that high angular resolution studies of polarization dependency confirm the conclusion made above on dramatically different polarization behaviors of the central crossbar junction and specific hot spots formed by nanoparticle–nanowire junctions.

CONCLUSIONS

In conclusion, we demonstrated that depending upon the exact location and orientation of decorating nanoparticles, a variety of different rotational patterns with different on/off SERS intensities can be designed. Overall, this approach provides means for the fabrication of arrays of hot spots that can be activated only at a certain polarization direction and suppressed at an orthogonal direction while keeping some hot spots activated under any condition. Such an array with on-demand activation could be of interest for multifunctional assays for chemical and biological detections. Although carrying out the exact placement of nanoparticles is challenging, we suggest that the proper design of crossbars decorated with nanoparticles might be completed by selective micropatterning, as will be a subject of future studies.

EXPERIMENTAL SECTION

Synthesis of Silver Nanowires. Silver nanowires were synthesized according to the polyol method introduced by Xia et al. using silver nitrate as the precursor, poly(vinylpyrrolidone) (0.36 M concentration and molecular weight, $M_n = 1\,300\,000\text{ g mol}^{-1}$) as the capping agent, and ethylene glycol as the solvent and reducing agent.³³ A solution (60 mL) of PVP in ethylene glycol was heated at 160°C under constant stirring for 1 h. Next, a separate solution (30 mL) of silver nitrate in ethylene glycol (AgNO_3 , 0.12 M) was prepared at room temperature with vigorous stirring. $\text{Fe}_{(\text{acac})_3}$ (50 μg) in ethylene glycol solution (0.5 mL) was added to the hot PVP solution, followed by dropwise addition of the homogeneous silver nitrate solution. The solution mixture was stirred for 1 h, or until the solution turned opaque gray. The formation of silver nanowires could be easily confirmed from an optical microscope with $20\times$ or $50\times$ objectives, which is best observed in the dark-field mode. The product is a mixture of silver nanowires and spherical nanoparticles. The silver nanowires were mostly isolated from spherical nanoparticles by multiple centrifugation (3300 rpm) and redispersion in methanol. For the purpose of this experiment, the silver nanowires were only exposed to the centrifugation and redispersion cycle twice to maintain a certain concentration of spherical silver nanoparticles, which gives a silver nanowire/spherical nanoparticle mixture.

Fabrication of the Crossbar Arrays of Silver Nanowires. To prepare crossbar arrays of silver nanowires on silicon substrate, sacrificial polystyrene (PS) micropatterns (Janssen Chimica, $M_w = 250\,000$) was used as guided templates for the deposition of silver nanowires. We first drop-casted silver nanowire solution (1–3 mg/mL in methanol) onto the array of narrow channels composed of a sacrificial PS micropattern (ridges with 3 μm periodicity and 1 μm height) to prepare parallel arrays of silver nanowires. The 1 μm thick sacrificial PS micropattern is

deposited on silicon substrate by a PDMS stamp. After deposition of silver nanowires, the PS pattern was lifted off by toluene, leaving patterned stripe arrays of silver nanowires. We repeated the process of PS micropatterns perpendicular to the first layer of silver nanowire arrays to prepare crossed arrays of silver nanowires.

Raman Mapping of the Crossbar Array of Silver Nanowires. Confocal Raman mapping of crossbar arrays of silver nanowires with the highest resolution ($360\text{ nm} \times 360\text{ nm}$ spot size, 1.7 mW) at peak of 1600 cm^{-1} was conducted at different polarization directions ($0^\circ, 45^\circ, 90^\circ, 135^\circ, 180^\circ$) (Alpha300R Witek confocal Raman microscope) with an argon ion laser, $\lambda = 514.5\text{ nm}$, with the incident power set within $1\text{--}3\text{ mW}$.⁴⁸

SEM of the Crossbar Array of Silver Nanowires. A field-emission scanning electron microscope (FESEM, LEO 1530) was used to investigate the morphology of crossbars of silver nanowires. Dark-field optical images of crossbars and orthogonal silver nanowire arrays were obtained using a LEICA Microsystem DM4000 microscope.

AFM of the Crossbar Array of Silver Nanowires. AFM scanning was conducted to show the morphology of the silver nanowires on a Dimension 3000-Nanoscope IIIa microscope (Digital Instruments). AFM images were collected in the tapping mode according to the procedure adapted in our laboratory.^{49,50} AFM images of at least several different areas on the crossbar arrays of silver nanowires were obtained and the representative image of silver nanowires was selected. Silicon nitride tips were used with spring constants ranging from 0.01 to 50 N m^{-1} and tip radii between 20 and 50 nm . AFM scanning was conducted with the rate of $0.8\text{--}1.0\text{ Hz}$.

AUTHOR INFORMATION

Corresponding Author

*E-mail: vladimir@mse.gatech.edu.

ACKNOWLEDGMENT

The authors acknowledge generous support from NSF-CBET, AFOSR, EngeniusMicro, LLC, and DARPA and thank Prof. S. Singamaneni and Dr. R. Kodiyath for helpful discussions.

REFERENCES

- (1) Quinten, M.; Leitner, A.; Krenn, J. R.; Aussenegg, F. R. *Opt. Lett.* **1998**, *23*, 1331.
- (2) Takahara, J.; Yamagishi, S.; Taki, H.; Morimoto, A.; Kobayashi, T. *Opt. Lett.* **1997**, *22*, 475.
- (3) Jackson, J. B.; Halas, N. J. *Proc. Natl. Acad. Sci. U. S. A.* **2004**, *101*, 17930.
- (4) Ko, H.; Singamaneni, S.; Tsukruk, V. V. *Small* **2008**, *4*, 1576.
- (5) Yoshida, K.-I.; Itoh, T.; Tamaru, H.; Biju, V.; Ishikawa, M.; Ozaki, Y. *Phys. Rev. B* **2010**, *81*, 115406.
- (6) Moskovits, M. *Rev. Mod. Phys.* **1985**, *57*, 783.
- (7) Vo-Dinh, T.; Dhawan, A.; Norton, S. J.; Khouri, C. G.; Wang, H.-N.; Misra, V.; Gerhold, M. D. *J. Phys. Chem. C* **2010**, *114*, 7480.
- (8) Xu, H.; Aizpurua, J.; Käll, M.; Apell, P. *Phys. Rev. E* **2000**, *62*, 4318.
- (9) Halas, N. J. *Nano Lett.* **2010**, *10*, 3816.
- (10) Banholzer, M. J.; Millstone, J. E.; Qin, L.; Mirkin, C. A. *Chem. Soc. Rev.* **2008**, *37*, 885.
- (11) Willets, K.; Van Duyne, R. P. *Annu. Rev. Phys. Chem.* **2007**, *58*, 267.
- (12) Lyvers, D. P.; Moon, J. M.; Kildishev, A. V.; Shalaev, V. M.; Wei, A. *ACS Nano* **2008**, *2*, 2569.
- (13) Ko, H.; Tsukruk, V. V. *Small* **2008**, *4*, 1980.
- (14) Chang, S.; Combs, Z. A.; Gupta, M.; Davis, R.; Tsukruk, V. V. *ACS Appl. Mater. Interfaces* **2010**, *2*, 3333.
- (15) Ko, H.; Chang, S.; Tsukruk, V. V. *ACS Nano* **2009**, *3*, 181.
- (16) Chang, S.; Ko, H.; Singamaneni, S.; Gunawidjaja, R.; Tsukruk, V. V. *Anal. Chem.* **2009**, *81*, 5740.
- (17) Yoon, I.; Kang, T.; Choi, W.; Kim, J.; Yoo, Y.; Joo, S.-W.; Park, Q.-H.; Ihhee, H.; Kim, B. *J. Am. Chem. Soc.* **2009**, *131*, 758.
- (18) Tao, A.; Kim, F.; Hess, C.; Goldberger, J.; He, R.; Sun, Y.; Xia, Y.; Yang, P. *Nano Lett.* **2003**, *3*, 1229.
- (19) Lee, S. J.; Morrill, A. R.; Moskovits, M. *J. Am. Chem. Soc.* **2006**, *128*, 2200.
- (20) Mahmoud, M. A.; Tabor, C. E.; El-Sayed, M. A. *J. Phys. Chem. C* **2009**, *113*, 5493.
- (21) Gunawidjaja, R.; Kharlampieva, E.; Choi, I.; Tsukruk, V. V. *Small* **2009**, *5*, 2460.
- (22) Chen, X.; Jeon, Y.-M.; Jang, J.-W.; Qin, L.; Huo, F.; Wei, W.; Mirkin, C. A. *J. Am. Chem. Soc.* **2008**, *130*, 8166.
- (23) Lim, D.-K.; Jeon, K.-S.; Kim, H.-M.; Nam, J.-M.; Suh, Y. D. *Nat. Mater.* **2010**, *9*, 60.
- (24) Kang, T.; Yoo, S. M.; Yoon, I.; Lee, S. Y.; Kim, B. *Nano Lett.* **2010**, *10*, 1189.
- (25) Kang, T.; Yoon, I.; Kim, J.; Ihhee, H.; Kim, B. *Chem.—Eur. J.* **2010**, *16*, 1351.
- (26) Yoon, H. P.; Maitani, M. M.; Cabarcos, O. M.; Cai, L.; Mayer, T. S.; Allara, D. L. *Nano Lett.* **2010**, *10*, 2897.
- (27) Cheng, C.; Yan, B.; Wong, S. M.; Li, X.; Zhou, W.; Yu, T.; Shen, Z.; Yu, H.; Fan, H. *J. ACS Appl. Mater. Interfaces* **2010**, *2*, 1824.
- (28) Qi, H.; Alexson, D.; Glembotck, O.; Prokes, S. M. *Nanotechnology* **2010**, *21*, 215706.
- (29) Gunawidjaja, R.; Peleshanko, S.; Ko, H.; Tsukruk, V. V. *Adv. Mater.* **2008**, *20*, 1544.
- (30) Lee, S. J.; Baik, J. M.; Moskovits, M. *Nano Lett.* **2008**, *8*, 3244.
- (31) Ko, H.; Jiang, C.; Tsukruk, V. V. *Chem. Mater.* **2005**, *17*, 5489.
- (32) Weintraub, B.; Chang, S.; Singamaneni, S.; Han, W. H.; Choi, Y. J.; Bae, J.; Kirkham, M.; Tsukruk, V. V.; Deng, Y. *Nanotechnology* **2008**, *19*, 435302.
- (33) Sun, Y. G.; Gates, B.; Mayers, B.; Xia, Y. *Nano Lett.* **2002**, *2*, 165.
- (34) Gunawidjaja, R.; Jiang, C.; Peleshanko, S.; Ornatska, M.; Singamaneni, S.; Tsukruk, V. V. *Adv. Funct. Mater.* **2006**, *16*, 2024.
- (35) Fang, Y.; Wei, H.; Hao, F.; Nordlander, P.; Xu, H. *Nano Lett.* **2009**, *9*, 2049.
- (36) Hutchison, J. A.; Centeno, S. P.; Odaka, H.; Fukumura, H.; Hofkens, J.; Uji-I, H. *Nano Lett.* **2009**, *9*, 995.
- (37) Wei, H.; Hao, F.; Huang, Y.; Wang, W.; Nordlander, Xu, H. *Nano Lett.* **2008**, *8*, 2497.
- (38) Jiang, C.; Tsukruk, V. V. *Soft Matter* **2005**, *1*, 334.
- (39) Gole, A.; Murphy, C. J. *Langmuir* **2005**, *21*, 10756.
- (40) Gao, Y.; Jiang, P.; Liu, D. F.; Yuan, H. J.; Yan, X. Q.; Zhou, Z. P.; Wang, J. X.; Song, L.; Liu, L. F.; Zhou, W. Y.; Wang, G.; Wang, C. Y.; Xie, S. S.; Zhang, J. M.; Shen, D. Y. *J. Phys. Chem. B* **2004**, *108*, 12877.
- (41) Ko, H.; Tsukruk, V. V. *Nano Lett.* **2006**, *6*, 1443.
- (42) Borodko, Y.; Habas, S. E.; Koebel, M.; Yang, P.; Frei, H.; Somorjai, G. A. *J. Phys. Chem. B* **2006**, *110*, 23052.
- (43) Ferrari, A. C.; Robertson J. *Phys. Rev. B* **2000**, *61*, 14095.
- (44) Schwan, J.; Ulrich, S.; Batori, V.; Ehrhardt, H.; Silva, S. R. P. J. *Appl. Phys.* **1996**, *80*, 440.
- (45) Ferrari, A. C.; Robertson, J. *Philos. Trans. R. Soc. London, Ser. A* **2004**, *362*, 2477.
- (46) Aroca, R. *Surface-Enhanced Vibrational Spectroscopy*; John Wiley & Sons: Chichester, 2006.
- (47) Tran, M. L.; Centeno, S. P.; Hutchison, J. A.; Engelkamp, H.; Liang, D.; Tendeloo, G. V.; Sels, B. F.; Hofkens, J.; Uji-I, H. *J. Am. Chem. Soc.* **2008**, *130*, 17240.
- (48) Singamaneni, S.; Gupta, M.; Yang, R.; Tomczak, M. M.; Naik, R. R.; Wang, Z. L.; Tsukruk, V. V. *ACS Nano* **2009**, *3*, 2593.
- (49) Tsukruk, V. V. *Rubber Chem. Technol.* **1997**, *70*, 430.
- (50) McConney, M. E.; Singamaneni, S.; Tsukruk, V. V. *Polym. Rev.* **2010**, *50*, 235.